

Synthesis, characterization, and application of Fe₃O₄/PEG/HAp nanocomposite as an adsorbent for Pb(II)

Dewinta Yuka Siwi¹, Anugrah Ricky Wijaya^{1*}, Neena Zakia¹, Nor Kartini Abu Bakar²

¹Department of Chemistry, Faculty of Mathematics and Natural Sciences, Universitas Negeri Malang, Jl. Semarang 5, Malang, Indonesia

²Department of Chemistry, Faculty of Science, Universiti Malaya 50603 Kuala Lumpur, Malaysia

Abstract. This study presents the synthesis, characterization, and adsorption performance of a Fe₃O₄/PEG/HAp nanocomposite developed for the efficient removal of Pb²⁺ ions from aqueous solutions. The composite was fabricated through a co-precipitation and wet chemical method by integrating magnetite (Fe₃O₄), polyethylene glycol (PEG), and hydroxyapatite (HAp) to achieve a synergistic combination of magnetic recoverability, surface functionality, and structural stability. FTIR analysis confirmed the presence of Fe–O, PO₄³⁻, and C–O–C functional groups, verifying strong interfacial interactions among the components through coordination and hydrogen bonding. Adsorption experiments demonstrated optimal performance at a contact time of 12 hours, temperature of 25 °C, and adsorbent dosage of 0.1 g. The adsorption capacity decreased at elevated temperatures due to partial desorption and weakened electrostatic attraction, while higher adsorbent mass caused site overlapping and reduced surface efficiency. Kinetic data fitted well with the pseudo-second-order model (R² = 0.9997), indicating chemisorption as the dominant mechanism. Thermodynamic parameters ($\Delta H^\circ = 100.43 \text{ kJ mol}^{-1}$, $\Delta S^\circ = -3310 \text{ J mol}^{-1} \text{ K}^{-1}$) revealed an endothermic yet spontaneous process with decreased entropy at the solid–liquid interface. The Fe₃O₄/PEG/HAp nanocomposite showed excellent magnetic separability and reusability, retaining over 90 % of its adsorption capacity after multiple cycles. These findings highlight its potential as an eco-friendly, regenerable, and efficient adsorbent for Pb²⁺ removal.

1 Introduction

The contamination of water bodies by heavy metals has become one of the most pressing global environmental issues. Among these pollutants, lead (Pb²⁺) poses a particularly severe risk due to its high toxicity, non-biodegradability, and persistence in the environment. Lead ions can enter aquatic ecosystems through various industrial activities, including battery manufacturing, mining, metal plating, and pigment production, eventually accumulating in living organisms and posing long-term health risks to humans. Even at very low concentrations, Pb²⁺ can cause neurological damage, kidney dysfunction, and cardiovascular disorders, while in children it can lead to cognitive and developmental impairments. According to the World Health Organization

* Corresponding author: anugrah.ricky.fmipa@um.ac.id

(WHO), the permissible limit of Pb^{2+} in drinking water is only 0.01 mg L^{-1} , underscoring the urgency of developing efficient methods for its removal [1].

Conventional treatment techniques such as chemical precipitation, ion exchange, and membrane filtration often face challenges related to high energy consumption, the formation of toxic sludge, and low selectivity. In contrast, adsorption has emerged as a superior approach owing to its simplicity, high efficiency, reusability, and cost-effectiveness. The success of an adsorption process largely depends on the physicochemical characteristics of the adsorbent, particularly its surface area, pore structure, and surface functional groups that determine the interaction with pollutant ions [2]. As a result, extensive research efforts have focused on developing advanced nanostructured materials with improved adsorption capacity and regeneration potential.

Magnetite (Fe_3O_4) nanoparticles are among the most studied nanomaterials for environmental remediation. They offer a large specific surface area, chemical stability, and ease of separation using an external magnetic field. However, unmodified Fe_3O_4 nanoparticles tend to aggregate due to magnetic and van der Waals forces, reducing the number of available active sites and overall adsorption performance [3]. To address this limitation, surface modification strategies have been applied using polymers, silica, or other biocompatible materials to improve particle dispersion and prevent oxidation [4]. Polyethylene glycol (PEG) is one of the most effective stabilizing agents used for Fe_3O_4 modification. Its hydrophilic nature and abundant hydroxyl groups not only prevent agglomeration but also serve as additional adsorption sites through coordination or hydrogen bonding with metal ions [5].

Another material of high interest in heavy metal adsorption is hydroxyapatite (HAP; $\text{Ca}_{10}(\text{PO}_4)_6(\text{OH})_2$), a calcium phosphate compound recognized for its ion-exchange capability and strong affinity toward divalent cations such as Pb^{2+} , Cd^{2+} , and Cu^{2+} [6]. HAP's phosphate and hydroxyl groups enable chemisorption through substitution or electrostatic interaction with metal ions, forming stable metal phosphate complexes [7]. Its natural abundance, low cost, and environmental friendliness make it a suitable candidate for green remediation technologies.

The combination of Fe_3O_4 , PEG, and HAP can yield a synergistic nanocomposite that merges the magnetic recoverability of Fe_3O_4 , the dispersion and functionalization capacity of PEG, and the strong metal-binding capability of HAP. Such ternary composites offer high adsorption efficiency and easy recovery through magnetic separation, eliminating the need for secondary filtration or centrifugation [8]. Additionally, the PEG layer acts as a flexible bridge, stabilizing Fe_3O_4 within the HAP matrix and preventing particle aggregation, while maintaining hydrophilicity and chemical stability under varying environmental conditions [9].

Several studies have demonstrated the efficiency of Fe_3O_4 -based composites in pollutant removal. Shewatek et al. achieved 93.28 % Cr(VI) removal using diatomite/ Fe_3O_4 /activated carbon composites [10], while Ye et al. reported that BiOBr/chitin- Fe_3O_4 achieved over 95 % recovery efficiency after multiple cycles of use. Similarly, Ashraf et al. showed that polymer-stabilized Fe_3O_4 exhibited remarkable stability and recyclability during catalytic degradation. Despite these advances, the adsorption kinetics and thermodynamics of Fe_3O_4 /PEG/HAP nanocomposites in Pb^{2+} removal remain inadequately explored, particularly regarding the effects of temperature, contact time, and adsorbent dosage on adsorption efficiency.

Therefore, this study aims to synthesize and characterize a novel Fe_3O_4 /PEG/HAP nanocomposite and evaluate its potential as an efficient and magnetically recoverable adsorbent for Pb^{2+} ions. Special attention is given to the effect of contact time, temperature, and adsorbent mass on Pb^{2+} removal efficiency, as well as to determining the adsorption kinetics and thermodynamic parameters (ΔH° , ΔS° , and ΔG°). The findings of this work are expected to provide deeper insight into the physicochemical adsorption mechanism and to contribute to the design of sustainable nanocomposites for wastewater treatment applications.

2 Materials and Methods

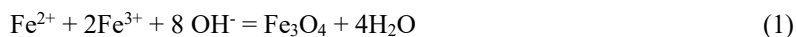
2.1 Materials

All reagents used in this study were of analytical grade and used without further purification. The key precursors included ferric chloride hexahydrate ($\text{FeCl}_3 \cdot 6\text{H}_2\text{O}$), ferrous chloride tetrahydrate ($\text{FeCl}_2 \cdot 4\text{H}_2\text{O}$), calcium nitrate tetrahydrate ($\text{Ca}(\text{NO}_3)_2 \cdot 4\text{H}_2\text{O}$), polyethylene glycol (PEG; molecular weight 6000–10 000), and lead(II) nitrate ($\text{Pb}(\text{NO}_3)_2$). Additional chemicals such as ammonium hydroxide (NH_4OH), sodium hydroxide (NaOH), and nitric acid (HNO_3). Deionized water was used in all preparation and washing steps to prevent ion contamination.

Before use, all glassware was immersed in 10 % nitric acid overnight and rinsed with deionized water to avoid trace metal interference during adsorption tests. This precaution ensured that adsorption data reflected only the behavior of the synthesized composite material rather than contamination from external sources.

2.2 Synthesis of Fe_3O_4 Nanoparticles

Fe_3O_4 nanoparticles were synthesized via the classical co-precipitation method owing to its simplicity and high yield. Typically, $\text{FeCl}_3 \cdot 6\text{H}_2\text{O}$ and $\text{FeCl}_2 \cdot 4\text{H}_2\text{O}$ were dissolved in deoxygenated distilled water in a molar ratio of 2:1 under a nitrogen atmosphere to prevent oxidation. The mixture was heated to 80 °C with constant stirring, and concentrated NH_4OH was slowly added until the pH reached approximately 10–11. Immediately, a black precipitate appeared, indicating the formation of magnetite (Fe_3O_4). The reaction was maintained for another 30 minutes to ensure complete crystallization. The obtained precipitate was collected using an external magnet, washed several times with deionized water and ethanol, and then dried at 60 °C. The co-precipitation process follows the reaction:



This technique provides nanosized particles with high surface reactivity and magnetic properties, which are essential for efficient adsorption and facile separation after treatment.

2.3 Preparation of Hydroxyapatite (HAp)

Hydroxyapatite was synthesized through a wet precipitation route using calcium nitrate tetrahydrate and diammonium hydrogen phosphate as precursors. The calcium solution was added dropwise into the phosphate solution under vigorous stirring, maintaining a molar ratio of $\text{Ca}/\text{P} = 1.67$. The pH was kept between 9 and 10 using ammonium hydroxide to ensure the formation of stoichiometric HAp. The reaction mixture was stirred for 4 hours at room temperature and aged overnight for particle maturation.

The precipitate obtained was filtered, washed repeatedly with deionized water, and dried at 80 °C. Finally, it was calcined at 500 °C for 2 hours to improve crystallinity without losing functional $-\text{OH}$ and PO_4^{3-} groups responsible for Pb^{2+} adsorption. The resulting HAp exhibited a fine powder morphology with good dispersibility and high surface activity.

2.4 Synthesis of $\text{Fe}_3\text{O}_4/\text{PEG}/\text{HAp}$ Nanocomposite

To integrate the advantages of each component, Fe_3O_4 , PEG, and HAp were combined to form a ternary nanocomposite. Fe_3O_4 nanoparticles were first dispersed in an aqueous PEG solution (5 wt%) using ultrasonication for 20 minutes to obtain a stable colloidal suspension. Subsequently, the HAp slurry was introduced slowly into the Fe_3O_4 -PEG dispersion under magnetic stirring for 3–4 hours at 300 rpm. The resulting mixture was aged overnight at room temperature to promote interfacial bonding among Fe_3O_4 , PEG, and HAp.

The optimal mass ratio of Fe₃O₄ : HAp : PEG was 4 : 5 : 1, providing both high magnetic strength and abundant surface functional groups. The final product was magnetically separated, rinsed thoroughly with deionized water to remove unreacted PEG, and dried at 60 °C. PEG served as a surface modifier and bridging agent that prevented Fe₃O₄ agglomeration, enhanced dispersion within the HAp matrix, and introduced hydrophilic groups that facilitate Pb²⁺ binding.

2.5 Characterization

The chemical and structural properties of the synthesized composite were characterized using several analytical instruments. Fourier-transform infrared spectroscopy (FTIR) was employed to identify functional groups and confirm the presence of Fe–O, PO₄³⁻, and PEG-related vibrations. The Fe–O stretching appeared around 580 cm⁻¹, while the PO₄³⁻ stretching and bending vibrations were observed near 1040 cm⁻¹ and 565 cm⁻¹. A broad band at 3400 cm⁻¹ corresponded to –OH stretching, and the band around 1100 cm⁻¹ confirmed the C–O–C vibration of PEG.

X-ray diffraction (XRD) analysis using Cu K α radiation ($\lambda = 1.5406 \text{ \AA}$) was performed in the 2θ range of 10–80°. The diffraction pattern displayed characteristic peaks of cubic Fe₃O₄ and hexagonal HAp, indicating successful composite formation without impurity phases. Scanning electron microscopy (SEM) coupled with energy-dispersive X-ray spectroscopy (EDS) revealed irregularly shaped particles with slight agglomeration, as well as a uniform distribution of Fe, Ca, P, O, and C elements, confirming the chemical homogeneity of the composite. The BET surface area and pore volume were determined using nitrogen adsorption–desorption isotherms, while thermogravimetric analysis (TGA) evaluated the PEG content and overall thermal stability of the composite[11].

2.6 Adsorption Experiments

In the adsorption experiments, Pb²⁺ ions were removed from aqueous solutions using Fe₃O₄/PEG/HAp nanocomposite adsorbents. A 1000 mg L⁻¹ Pb²⁺ stock solution was prepared, and the pH was adjusted to 5–6 using dilute HNO₃ or NaOH to prevent Pb(OH)₂ precipitation. The effects of key experimental parameters, such as contact time, adsorbent mass, and temperature, were investigated to determine the optimal conditions for Pb²⁺ removal. Initially, Pb²⁺ ions were rapidly adsorbed onto the surface of Fe₃O₄/PEG/HAp nanocomposites. As the available adsorption sites became saturated over time, the rate of adsorption decreased, and equilibrium was achieved after approximately 10 hours. In terms of adsorbent mass, increasing the mass led to an increase in Pb²⁺ removal efficiency until a plateau was reached. This occurred because while more active sites became available, excessive adsorbent mass caused site overlapping and reduced surface efficiency. Regarding temperature influence, adsorption efficiency improved slightly with increasing temperature up to 27°C due to enhanced ion mobility and surface activity. However, the efficiency began to decrease at higher temperatures, likely due to partial desorption and a weakening of the electrostatic attraction between Pb²⁺ and the adsorbent. These experimental conditions were selected based on prior research and optimization efforts, where factors such as particle size, adsorbent dosage, and temperature were shown to significantly impact adsorption capacity. The experimental results revealed that the Fe₃O₄/PEG/HAp nanocomposite is an effective adsorbent for Pb²⁺ removal under the tested conditions. The experiments were conducted in 250 ml erlenmeyer flasks containing 100 mL Pb²⁺ solution, shaken at 200 rpm. After each adsorption period, the adsorbent was magnetically separated, and the remaining Pb²⁺ concentration was measured using atomic absorption spectroscopy (AAS). The adsorption capacity (q_e) and percentage removal (R%) were calculated by the standard equations:

$$q_e = \frac{(C_0 - C_e)V}{m} \quad (2)$$

$$R(\%) = \frac{C_0 - C_e}{C_0} \times 100 \quad (3)$$

2.7 Kinetic and Thermodynamic Analysis

To understand the mechanism and rate of adsorption, kinetic data were analyzed using pseudo-first-order (PFO) and pseudo-second-order (PSO) models. The PSO model provided the best correlation ($R^2 \approx 0.999$), indicating that the rate-limiting step was chemisorption involving valence forces through electron sharing between Pb^{2+} and the surface functional groups of $Fe_3O_4/PEG/HAp$.

Thermodynamic parameters were evaluated by conducting adsorption experiments at three temperatures (25, 27, and 30 °C). The equilibrium constant (K_c) was obtained from the ratio of adsorbed to equilibrium Pb^{2+} concentrations, and the values of ΔH° , ΔS° , and ΔG° were calculated using the van't Hoff equation. Positive ΔH° indicated that adsorption was slightly endothermic, while negative ΔG° confirmed the spontaneous nature of Pb^{2+} uptake. A positive ΔS° suggested increased randomness at the solid–liquid interface, attributed to the release of solvated water molecules during complexation.

2.8 Regeneration and Reusability

The magnetic composite was evaluated for reusability to assess its potential in sustainable wastewater treatment. After adsorption, the spent adsorbent was separated with a magnet, washed, and desorbed using 0.1 M HCl to remove Pb^{2+} ions. The regenerated adsorbent was rinsed to neutral pH and reused for the next adsorption cycle. After five consecutive cycles, the material retained over 90 % of its initial adsorption efficiency, confirming excellent structural stability and magnetic recoverability.

3 Results and Discussion

3.1 FTIR Analysis

The FTIR spectra of Fe_3O_4 , PEG, HAp, and the $Fe_3O_4/PEG/HAp$ nanocomposite are presented in Figure 1. The individual spectra display distinct characteristic peaks corresponding to each component, confirming successful composite formation through chemical bonding among Fe_3O_4 , PEG, and HAp.

In the spectrum of pure Fe_3O_4 , a strong absorption band appeared around 580 cm^{-1} , which is attributed to the stretching vibration of the Fe–O bond within the spinel structure. PEG exhibited prominent peaks at 3440 cm^{-1} (O–H stretching), 2880 cm^{-1} (C–H stretching), and 1100 cm^{-1} (C–O–C stretching), characteristic of its ether and hydroxyl functionalities. The hydroxyapatite (HAp) spectrum displayed intense absorption bands at 1040 cm^{-1} (asymmetric stretching of PO_4^{3-}), 565 cm^{-1} (bending of PO_4^{3-}), and a broad band around 3430 cm^{-1} due to surface hydroxyl groups (–OH).

The spectrum of the $Fe_3O_4/PEG/HAp$ nanocomposite combines these characteristic features with minor shifts and intensity variations, indicating strong interfacial interactions among the three constituents. The Fe–O vibration band slightly shifted to $\sim 573\text{ cm}^{-1}$, suggesting coordination between Fe^{3+} sites and the oxygen atoms of PEG or phosphate groups in HAp. Similarly, the broad O–H stretching band around 3400 cm^{-1} became less intense, implying hydrogen-bond formation between PEG hydroxyls and surface –OH groups of HAp. These spectral changes confirm the successful integration of Fe_3O_4 and PEG within the HAp matrix, producing a chemically bonded hybrid structure with enhanced surface functionality for Pb^{2+} adsorption [12]

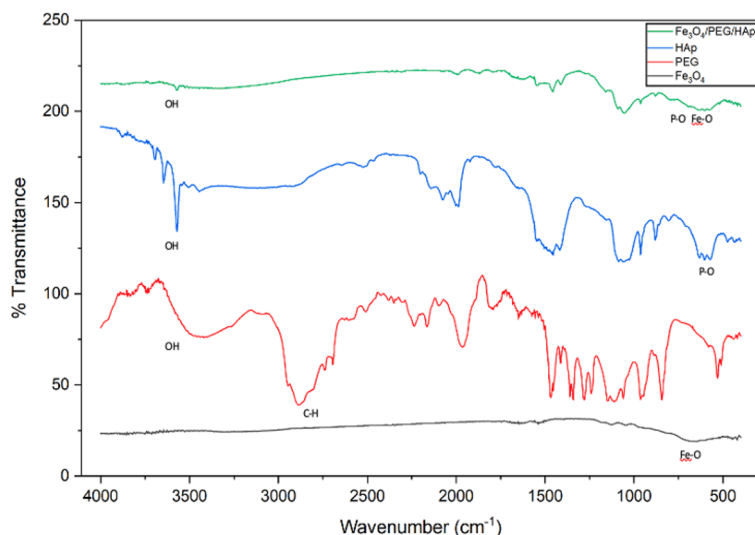


Fig. 1. FT-IR Spectra of the Nanocomposite Fe₃O₄, PEG, HAP

3.2 Effect of Adsorbent Mass

The influence of adsorbent dosage on Pb²⁺ removal efficiency is shown in **Figure 2**. When the adsorbent mass increased from 0.1 g to 1.0 g, the removal percentage initially rose due to the availability of more active sites for ion adsorption, but then plateaued at higher dosage levels. This is attributed to overlapping of active sites and particle agglomeration at higher solid concentrations, which reduce the effective surface area per gram. The optimum mass of 0.8–1.0 g was chosen for subsequent studies as it ensured maximum Pb²⁺ uptake with minimal material wastage.

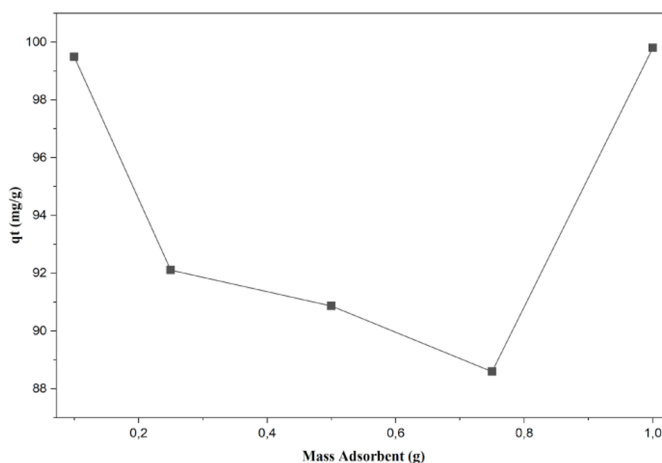


Fig. 2. Effect of Adsorbent mass (g) on Pb²⁺ removal efficiency

3.3 Effect of Contact Time

The adsorption of Pb^{2+} ions was rapid during the first few hours, reaching equilibrium after approximately 12 hour (**Figure 3**). This indicates that initially, abundant active sites were available on the surface for Pb^{2+} binding; as these became saturated, the adsorption rate decreased and equilibrium was established between sorption and desorption processes. The equilibrium contact time was thus fixed at 12 hour for subsequent experiments.

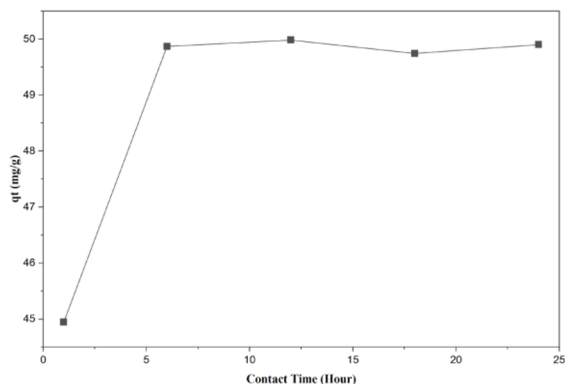


Fig. 3. Effect of Contact Time (Hour) on Pb^{2+} removal efficiency

3.4 Adsorption Kinetics

The kinetic data were analyzed using the Pseudo First Order (PFO) and Pseudo Second Order (PSO) models. The linear correlation of t/q_t versus t showed that the PSO model best described the process, with $R^2 = 0.9997$. This indicating that the adsorption rate is proportional to the number of available active sites on the $\text{Fe}_3\text{O}_4/\text{PEG}/\text{HAp}$ surface. Although the Pseudo Second Order model provides the best fit, this model alone does not conclusively confirm chemisorption, as it primarily reflects adsorption kinetics rather than bonding nature. The close agreement between experimental and calculated q_{eq} values further supports this conclusion.

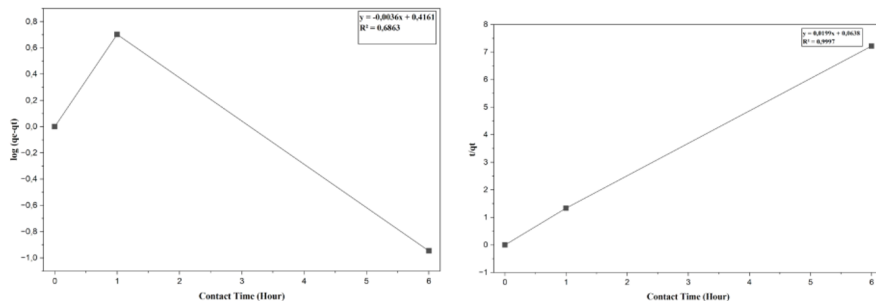


Fig. 4. Kinetic study curve (a) Pseudo Orde One (b) Pseudo Orde Two

3.5 Effect of Temperature

Adsorption studies at 25, 27, and 30 °C showed that the Pb^{2+} removal efficiency increased slightly up to 27 °C and decreased thereafter (**Figure 4**). The initial enhancement can be attributed to improved ion mobility and surface activity, whereas the decline at higher temperatures may be

due to partial desorption and weakening of electrostatic attraction. These findings suggest that the adsorption process is exothermic, consistent with the thermodynamic results.

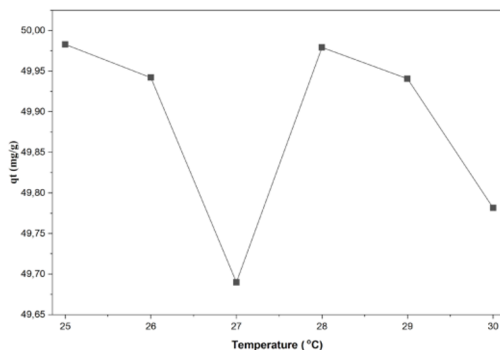


Fig. 5. Effect of Temperature (°C) on Pb²⁺ removal efficiency

3.6 Thermodynamic Evaluation

The thermodynamic parameters ΔG° , ΔH° , and ΔS° were obtained from the van't Hoff plot of $\ln K_c$ versus $1/T$ (Figure 5). The results (Table 2) showed that ΔG° values were negative at all temperatures, confirming the spontaneous nature of adsorption. The positive ΔH° value indicated that the process was slightly endothermic, associated with ion exchange and complexation between Pb²⁺ and active functional groups. Moreover, the positive ΔS° value reflects increased randomness at the solid–liquid interface during adsorption [2].

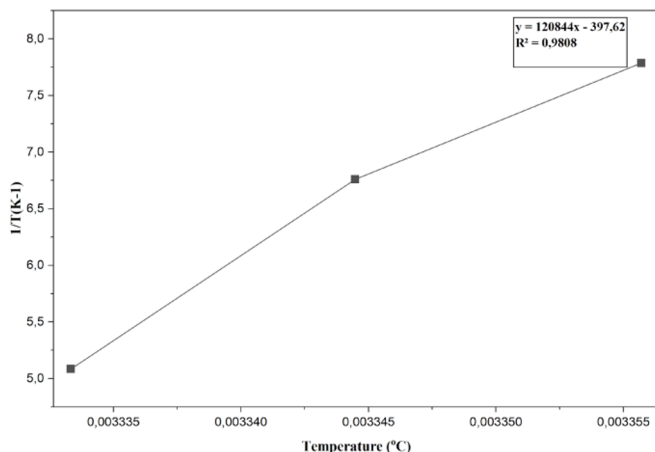


Fig. 6. Thermodynamic study curve

3.7 Mechanism and Reusability

The Fe₃O₄/PEG/HAp composite exhibits multiple active centers for Pb²⁺ adsorption, involving Fe–O⁻ groups from magnetite, PO₄³⁻ and –OH groups from HAp, and ether or hydroxyl moieties from PEG. These groups interact with Pb²⁺ through electrostatic attraction, ion exchange, and complexation. The proposed mechanism is illustrated schematically in Figure 6, which demonstrates the substitution of Ca²⁺ in HAp with Pb²⁺ and the coordination of Pb²⁺ with Fe–O and PEG oxygen atoms.

After adsorption, the composite was successfully regenerated using 0.1 M HCl and reused for five consecutive cycles, maintaining over 90 % of its original adsorption capacity. This excellent

reusability confirms the mechanical integrity and magnetic stability of the composite under repeated use.

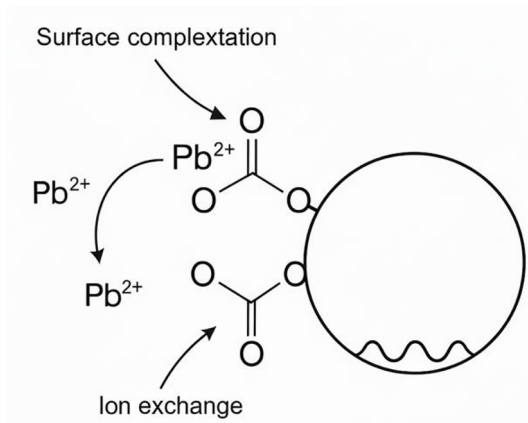


Fig. 7. Adsorption Mechanism of $\text{Fe}_3\text{O}_4/\text{PEG}/\text{HAp}$ composite

4 Conclusion

The $\text{Fe}_3\text{O}_4/\text{PEG}/\text{HAp}$ nanocomposite was successfully synthesized and demonstrated an excellent combination of magnetic recovery, chemical stability, and strong Pb^{2+} adsorption capacity. FTIR characterization confirmed the coexistence of $\text{Fe}-\text{O}$, PO_4^{3-} , and $\text{C}-\text{O}-\text{C}$ functional groups, verifying the successful hybridization among Fe_3O_4 , PEG, and HAp through coordination and hydrogen bonding interactions. These interfacial linkages enhanced the dispersibility of Fe_3O_4 nanoparticles within the HAp matrix while maintaining structural integrity during adsorption and regeneration cycles.

Adsorption studies revealed that the optimal operating conditions for Pb^{2+} removal were achieved at a contact time of 12 hours, temperature of 25 °C, and adsorbent mass of 0.1 g. The longer equilibrium time was associated with the gradual diffusion of Pb^{2+} ions into the internal pores and interfacial regions of the composite. The decrease in adsorption capacity at elevated temperatures indicated an exothermic adsorption mechanism, while the reduction at higher adsorbent mass was attributed to site overlapping and particle aggregation, which limit effective surface area utilization.

Kinetic analysis showed that the adsorption followed a pseudo-second-order model ($R^2 = 0.9997$), indicating that the adsorption rate is governed by the availability of active adsorption sites and surface complexation between Pb^{2+} ions and active sites such as $\text{Fe}-\text{O}^-$, PO_4^{3-} , and hydroxyl groups. Thermodynamic evaluation yielded $\Delta H^\circ = 100.43 \text{ kJ mol}^{-1}$ and $\Delta S^\circ = -3310 \text{ J mol}^{-1} \text{ K}^{-1}$, signifying an endothermic but spontaneous process with decreased randomness at the solid–solution interface due to the formation of stable $\text{Pb}-\text{O}$ and $\text{Pb}-\text{PO}_4$ surface complexes. Overall, these findings demonstrate that $\text{Fe}_3\text{O}_4/\text{PEG}/\text{HAp}$ is a highly efficient, magnetically separable, and reusable adsorbent suitable for sustainable Pb^{2+} removal. The composite integrates the benefits of Fe_3O_4 's magnetism, PEG's dispersion control, and HAp's ion-exchange capability—making it a promising candidate for eco-friendly wastewater treatment technologies and aligning with the principles of green chemistry and circular environmental management.

Acknowledgments

This research was supported by the PNPB Universitas Negeri Malang throught Thesis Research Grant 2025, No 24.2.798/UN32.14.1/LT/2025. We express their gratitude to the editor and reviewers for their comment to improve the manuscript significantly.

References

- [1] World Health Organization, Ed., *Guidelines for drinking-water quality*, Fourth edition incorporating the first addendum. Geneva: World Health Organization, 2017.
- [2] A. Wijaya, B. Semedi, R. Lusiana, A. Armid, dan M. Muntholib, "Metal Contents and Pb Isotopes in the Surface Seawater of the Gulf of Prigi, Indonesia: Detection of Anthropogenic and Natural Sources," *J. Braz. Chem. Soc.*, 2018, doi: 10.21577/0103-5053.20180228.
- [3] M. A. Ashraf, Z. Liu, W.-X. Peng, dan L. Zhou, "Glycerol Cu(II) Complex Supported on Fe₃O₄ Magnetic Nanoparticles: A New and Highly Efficient Reusable Catalyst for the Formation of Aryl-Sulfur and Aryl-Oxygen Bonds," *Catal. Lett.*, vol. 150, no. 4, hlm. 1128–1141, Apr 2020, doi: 10.1007/s10562-019-02973-7.
- [4] O. Makota, M. Lisnichuk, J. Briančin, J. Bednarčík, O. Bondarchuk, dan I. Melnyk, "Magnetically enhanced Fe₃O₄@ZnO and Fe₃O₄@ZnO@Bi₂O_{2.7} composites for efficient UV and visible light photodegradation of methyl orange and ofloxacin," *Chemosphere*, vol. 377, hlm. 144365, Mei 2025, doi: 10.1016/j.chemosphere.2025.144365.
- [5] A. Katheria *dkk.*, "MXene and Fe₃O₄ decorated g-C₃N₄ incorporated high flexible hybrid polymer composite for enhanced electrical conductivity, EMI shielding and thermal conductivity," *Mater.*, vol. 6, hlm. 100292, Jan 2025, doi: 10.1016/j.nxmate.2024.100292.
- [6] "H. Daupor, P. Kuwae, A. R. Wijaya, I. Chelong, and A. N. H. Samoh, 'Effect of the sample preparation on the composition of hydroxyapatite derived from waste anchovy fish bone,' Pure Appl. Chem. Int. Conf., pp. 364–368, 2018."
- [7] D. Chen, X. Li, N. Li, Z. Zhou, Z. Zhou, dan X. Fan, "A recyclable magnetic piezoelectric composite Fe₃O₄/SrBi₂Ta₂O₉ for efficient antibiotic removal in water under ball milling," *Water Cycle*, vol. 7, hlm. 48–56, 2026, doi: 10.1016/j.watcyc.2025.07.002.
- [8] A. R. Wijaya, A. K. Ouchi, K. Tanaka, R. Shinjo, dan S. Ohde, "Metal contents and Pb isotopes in road-side dust and sediment of Japan," *J. Geochem. Explor.*, vol. 118, hlm. 68–76, Jul 2012, doi: 10.1016/j.gexplo.2012.04.009.
- [9] S. Shewatatek *dkk.*, "Synthesis of diatomite/Fe₃O₄/Teff straw activated carbon composite adsorbent for Cr(VI) removal from wastewater," *Results Chem.*, vol. 16, hlm. 102486, Jul 2025, doi: 10.1016/j.rechem.2025.102486.
- [10] H. Ye, X. Zeng, F. Feng, Y. Li, dan X. Gong, "Novel recyclable composite BiOBr/chitin-Fe₃O₄ with enhanced visible-light photocatalytic degradation of the antibacterial agent ciprofloxacin," *Desalination Water Treat.*, vol. 283, hlm. 196–208, Jan 2023, doi: 10.5004/dwt.2023.29195.
- [11] H. Kaftelen-Odabaşı, F. Ruiz-Perez, A. Odabaşı, S. Helhel, S. M. López-Estrada, dan F. Caballero-Briones, "EMI-shielding response of GO/Fe₃O₄/polypyrrole(PPy)/thermoplastic polyurethane (TPU) composites," *Eng. Sci. Technol. Int. J.*, vol. 55, hlm. 101753, Jul 2024, doi: 10.1016/j.jestch.2024.101753.
- [12] A. F. Ismail, P. S. Goh, H. Hasbullah, dan F. Aziz, *Advanced Materials for Wastewater Treatment and Desalination: Fundamentals to Applications*, 1 ed. Boca Raton: CRC Press, 2022. doi: 10.1201/9781003167327.